

# COS FUV Detector Dark Rates During SMOV and Cycle 17

---

David Sahnou<sup>1</sup>, Thomas Ake<sup>2</sup>, Jason McPhate<sup>3</sup>, Steven Penton<sup>4</sup>, Wei Zheng<sup>1</sup>,  
and Charles D. (Tony) Keyes<sup>2</sup>

<sup>1</sup> *Department of Physics & Astronomy, Johns Hopkins University, Baltimore, MD*

<sup>2</sup> *Space Telescope Science Institute, Baltimore, MD*

<sup>3</sup> *Space Sciences Lab, University of California, Berkeley, CA*

<sup>4</sup> *CASA, University of Colorado, Boulder, CO*

October 07, 2011

---

## ABSTRACT

*As part of Servicing Mission Orbital Verification (SMOV) after the fifth Hubble Servicing Mission (SM4), the dark rate of the FUV detector of the Cosmic Origins Spectrograph (COS) was measured. This document provides a first look at the dark rate as a function of time and the position of HST in its orbit during SMOV and Cycle 17. We find that the dark rate has been constant with time for both segments, at  $< 1$  count/sec/cm<sup>2</sup> away from the SAA, consistent with prelaunch predictions. Early SMOV data taken at a higher than nominal gain showed features which have disappeared now that the high voltage has been adjusted downward. Several localized features that remain on segment B can be removed by applying appropriate pulse height screening to the data. An adjustment to the SAA model has been made to lower the background rate near the SAA.*

---

## **Contents:**

- The COS FUV Detector (page 2)
- Observing Program (page 2)
- Initial Background Measurements (page 5)
- Background After HV Adjustment (page 9)
- Calcos and the background (page 12)
- Change History for COS ISR 201 (page 13)
- References (page 13)
- Appendix (page 14)

## **1. The COS FUV Detector**

The COS FUV detector is a windowless, photon-counting microchannel plate (MCP) detector with two independently operable segments. A cross delay line (XDL) anode is used to collect photoelectrons from each MCP stack and determine the location of the incident photons. The anode output is digitized to  $16384 \times 1024$  pixels, although the active area is only about  $14300 \times 400$ . Detector data can be collected in TIME-TAG mode, where an (x,y) position and the pulse height (photon gain) are passed to the ground; or ACCUM mode, where only a two-dimensional histogram of the data is saved.

During normal operations, the high voltage on each of the two segments switches between two values: HVNOM, the full high voltage value used when collecting science data; and HVLOW, a lower value used when not observing. The latter value is low enough to prevent damage to the detector when passing through the South Atlantic Anomaly (SAA), but is close enough to HVNOM that the voltage can quickly be ramped up when it is time to collect data.

Background counts in the detector can come from a number of sources, including the radioactive decay of atoms in the MCP glass, charged particles from the environment, and scattered light from the optical system. Since this is a photon-counting detector, individual events that are identified in TIME-TAG mode as background events can be screened out during pipeline processing.

## **2. Observing Program**

### ***2.1 Observing Plan***

As part of COS Servicing Mission Orbital Verification (SMOV), measurements of the dark rate of the Far Ultraviolet (FUV) detector were made by collecting science data with the COS instrument shutter closed. The primary SMOV program for this activity was

COS-24 (program 11482 – Figure 1), which consisted of thirty 3250 second exposures. Since data collection for this program began soon after the FUV detector was turned on, there were two primary goals of the program: (1) to map the dark count rate as a function of time and of position in the orbit; and (2) to verify the nominal operation of the FUV detector and confirm that TIME-TAG data could be properly collected, saved, and processed. Thus, specific observation times were chosen in order to collect dark counts in a variety of orbit types, including those where: (1) HST grazed the edge of the SAA contour, and (2) HST recently passed through the SAA. These cases were included in order to determine the suitability of the SAA model, which matches that used for STIS.

Additional dark exposures were taken during SMOV as part of program 11356 during the initial detector high voltage (HV) ramp-up sequence, although most of these were taken at lower than nominal voltage.

As the SMOV dark program neared completion, the Cycle 17 dark exposures (program 11895 – Figure 2) began. For this program, five 1330 second dark exposures were taken each week, with no constraint on the orbital location of HST. As a result, the observations are more randomly scattered around the earth, and a week's darks are typically observed back-to-back. Since the long-term changes in dark rates are of interest, results from this program through October 2010 are also included in this ISR. This program is designed to track long-term changes of the background rate as a function of time.

A list of dark exposures that is affected by the SAA is given in the appendix.

## ***2.2 Orbital Track of Observations***

The orbital tracks of HST for SMOV dark program 11482 (Figure 1) were chosen by COS Instrument Scientists in consultation with the Mission Planners. As a result, the data taken was concentrated along the boundaries of the SAA in order to sample its edges.

# Program 11482

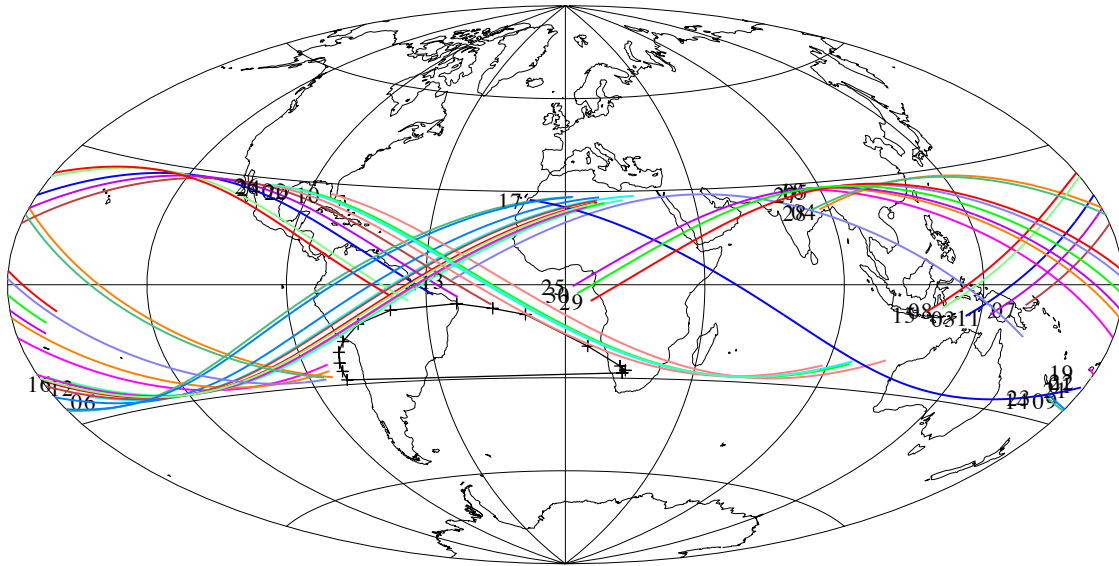


**Figure 1** HST ground track for exposures from program 11482. The colors are arbitrary; the labels note the visit number. Orbits are preferentially located near the SAA (marked with + symbols).

# Program 11895

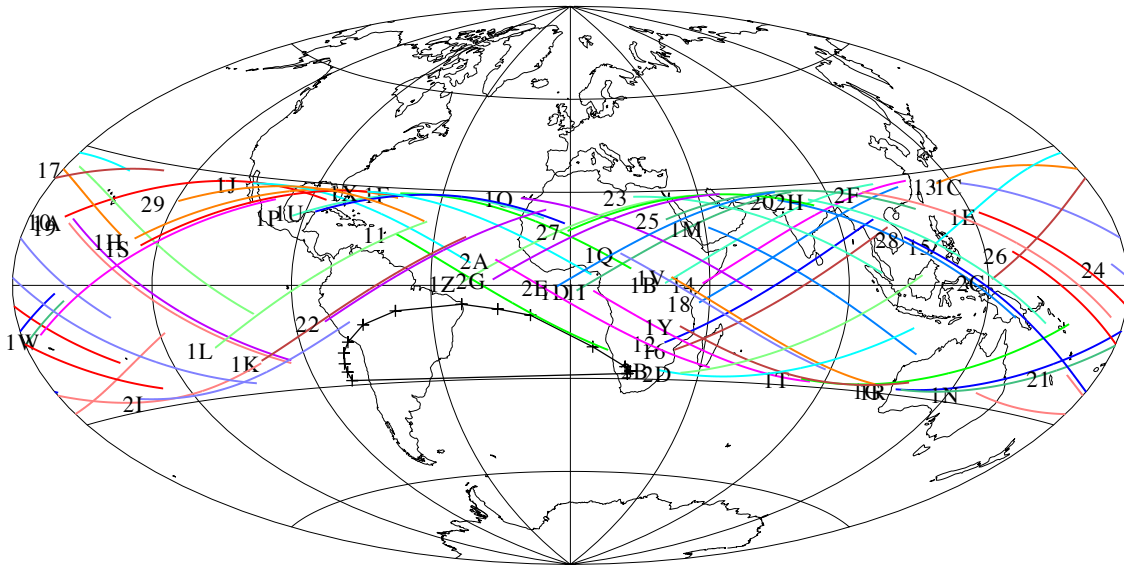


**Figure 2** HST ground track for exposures from program 11895 through 30 November 2009. These orbits are more randomly distributed than those in the previous figure. The colors are arbitrary; the labels identify the visit number.

## 3. Initial Background Measurements

### 3.1 Orbital Variation

#### 3.1.1 Science Data

All COS dark exposures are taken in TIME-TAG mode, and thus the count rate as a function of time and orbital position can be investigated using the science data. Plots of rate as a function of time (Figure 3) have been made for all background exposures. As expected, exposures which are taken while HST is near the SAA can have a significantly elevated background rate – up to a factor of 30 above the nominal value. The figure shows examples of count rate as a function of time on Segment A for two exposures in program 11482. The top panel (visit 12) shows data taken in an orbit with a grazing SAA passage (see Figure 1), while the bottom panel (visit 13) starts just after HST leaves the SAA.

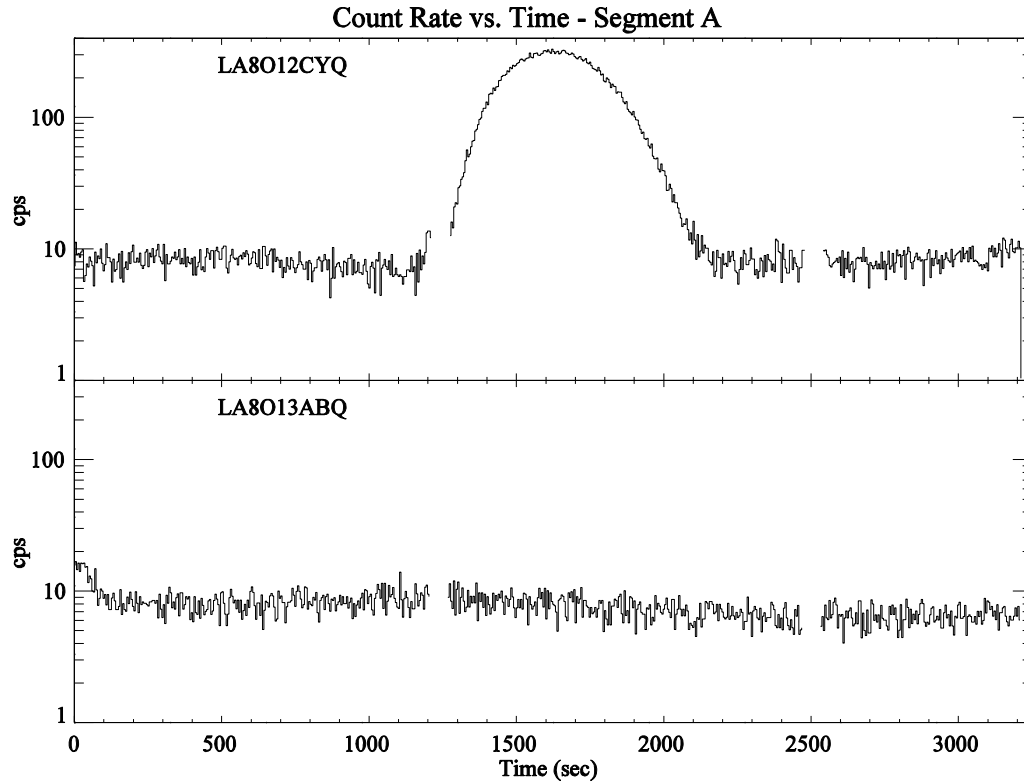


**Figure 3** Count rate as a function of time for two exposures in program 11482. The top panel shows an exposure during which HST’s orbit passes close to the COS SAA contour, and the total count rate on the detector reaches several hundred per second. The bottom panel shows the dark rate for an exposure which begins after HST leaves the SAA region.

This figure uses the pulse height thresholds of 4 and 30 (see Section 4.1), and includes only the counts on the active area of the detector, away from the edges.

### 3.1.2 Detector Counters

Whenever the FUV detector electronics is on, the detector electronics calculates several count rates for each segment. These counters include the Fast Event Counter (FEC), which is a measure of the total number of events reaching the detector’s microchannel plates. A one-second sample of the count rate is sent to the ground every 10 seconds as part of the instrument engineering data stream. Although count rates can only be calculated from the science data when an exposure is being taken, the engineering count rates are always available, except in the rare cases when the detector is turned off completely.

Although there is no simple correspondence between the count rates at HVLOW and HVNOM, the former can be used as a proxy for the latter in cases near the SAA, where the HVNOM count rates would be dangerous to the detector. Figure 4 shows the

measured count rate as a function of HST's latitude and longitude while segment A is at HVLOW. This map was built from data taken early in SMOV.

FUV LDCEFECA COUNTS AT HVLOW LEVEL

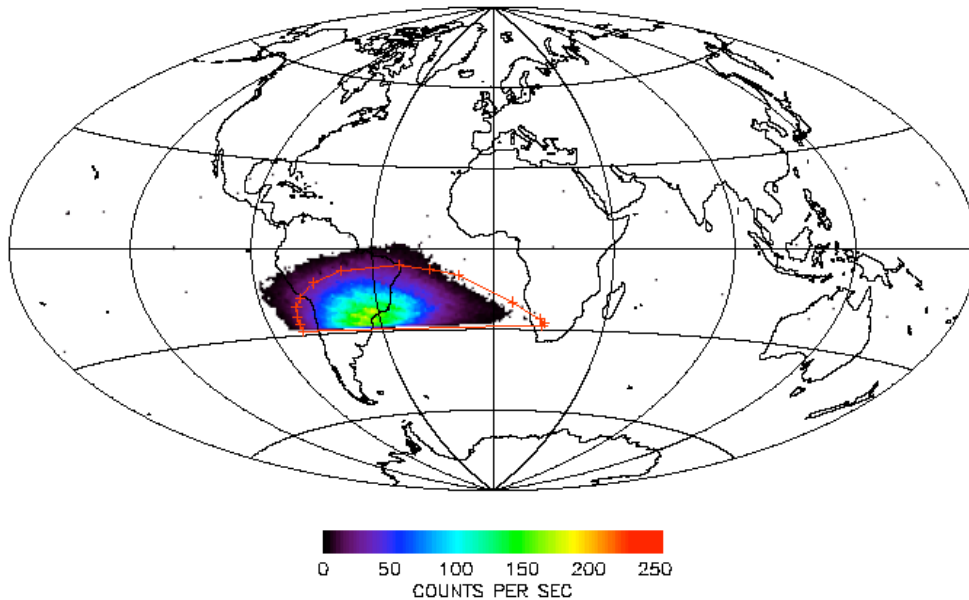


**Figure 4** Value of the FEC count rate on segment A as a function of orbital position, showing a large increase in counts when inside the SAA contour (marked by red + signs); segment B shows a similar effect. From this figure, it is clear that the original SAA model is offset from the actual SAA.

From the figure, it is apparent that the original SAA model (red plus signs) is not properly aligned with the measured detector count rate. This is consistent with the background rates seen in the science data, where enhanced count rates are seen on the western edge of the SAA, but not on the eastern side.

### 3.1.3 The SAA model and its effect on the data

As described in the previous sections, the shape and position of the initial SAA model did not match the dark measurements. Since the SAA is expected to change as a function of time due to variations in the solar cycle and short-term events on the sun (Furst et al., 2009), these changes should be made taking these variations into account.

By default, calcos subtracts a background based on the count rate measured on an unilluminated part of the detector (see Section 5. ), and for many applications, this will be sufficient. For the faintest targets, where having the lowest possible background is

desirable, data will be collected in TIME-TAG mode, and thus times of high background can be manually excluded by adjusting the Good Time Intervals (GTIs) in calcos. This is likely to result in the loss of only a small amount of data, since the time spent near the brightest part of the SAA is small during any orbit, and only one or two orbits a day is likely to be affected by a miscentered SAA model. In May 2010 a new SAA contour map was implemented for all instruments.

For ACCUM data it is not possible to screen data as a function of time, but since these targets are typically very bright, the effect of the higher background for a small portion of an exposure should be minimal.

### ***3.2 Spatial Distribution of Counts and HV adjustment***

The first examination of the SMOV quick-look sensitivity data during SMOV showed several features in spectra on segment B that were unexpected. Further investigation showed that these features were present in all data, and were stationary on the detector independent of the target observed or grating being used. Figure 5 shows an example of the two prominent features, dubbed the ‘divot’ and ‘clod’, in a sum of exposures from program 11484. These features had not been noticed in pre-launch data, but subsequent examination of data from prelaunch testing showed that they were sometimes present at a low level. These features were later shown to be due to the detector electronics misanalyzing high gain events due to precursor pulses triggering the time-to-digital converter (TDC) early (J. McPhate, COS-090731-JBM).

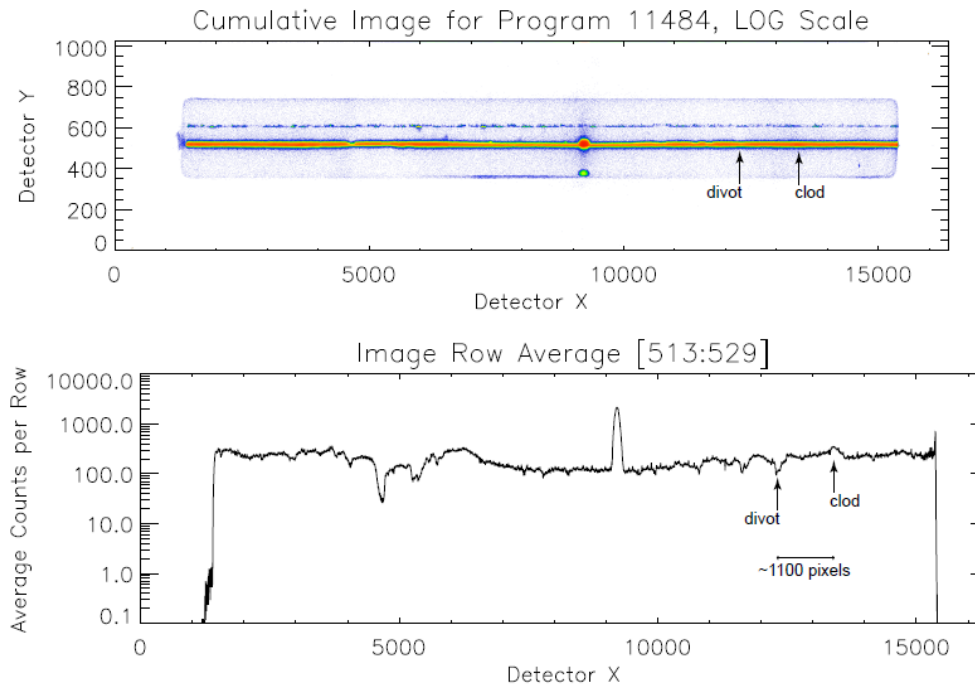


**Figure 5** Top: a coadded image of G130M and G160M segment B data from program 11484. Bottom: an extracted spectrum showing the divot and clod.

It was discovered during the initial HV ramp-up of the detector that the overall gain on both detector segments was approximately 20% higher than was seen on the ground at the same voltage levels. The exact reason for this difference is unclear, but it may be due to partially losing some of the detector scrub before launch. This increase in gain was enough to cause the divot and clod to be so noticeable.

In order to minimize the effects of these features, the high voltage on both segments was reduced on 12 August 2009 to return the gain to the values seen during ground testing (J. McPhate, COS TIR 2010-02). Subsequent examination of the data showed that the effects of the divot and clod were markedly reduced.

#### 4. Background After HV Adjustment

After the lowering of the high voltage, the divot and clod mostly disappeared, although several additional features were still visible in long darks, particularly on segment B. These features (top panels of Figure 6 and Figure 7) lie in the extraction region for the PSA and thus can have a substantial effect on the background at certain detector locations.

#### 4.1 Pulse Height Filtering

In addition to its (x,y) position, each photon event from the detector in TIME-TAG mode includes the pulse height, which is a measure of the gain of that event. Pulse heights range from 0 to 31. Calcos can filter on pulse height, but during SMOV and early Cycle 17, no pulse height screening was used. A study by UC Berkeley (J. McPhate, COS-090923-JBM) showed that including only pulse heights from 4 to 30 for both segments lowers the overall background and decreases the contribution from the features described above without having a large effect on the throughput.

The measurements in this ISR were made with a pulse range of 4 to 30. In order to minimize the effects of detector gain sag, the lower threshold was decreased to 2 in late 2010. This change increased the measured dark rate by approximately 7%.

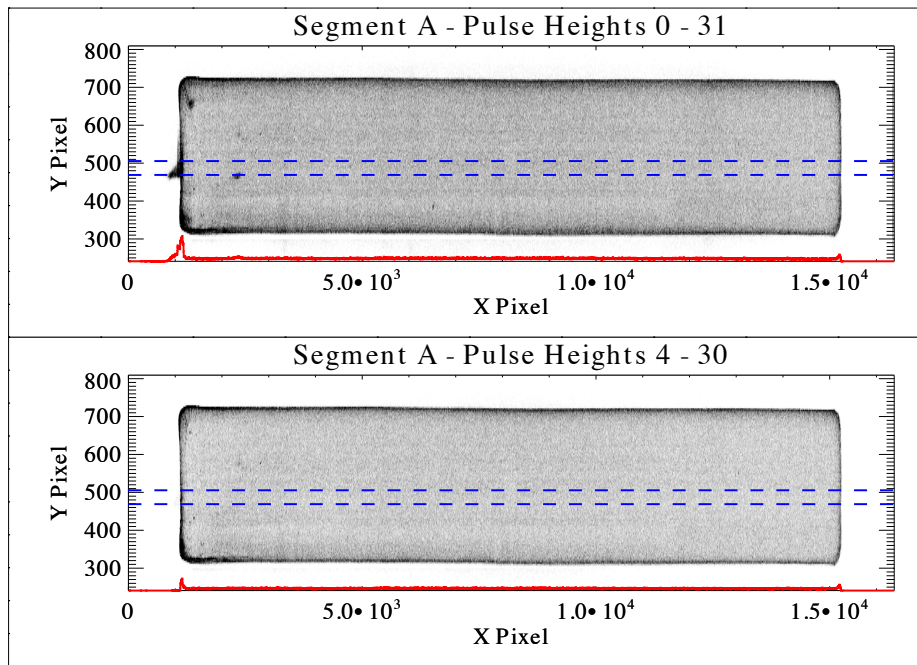


**Figure 6** Segment A background image with all pulse heights included (top) and with only pulse heights 4 to 30 (bottom), for a sum of ~19,000 seconds of background taken away from the SAA. A projection of the two dimensional data (red) in the region extracted for the G130M,  $\lambda_c=1309$  setting (marked by blue lines) is also shown.

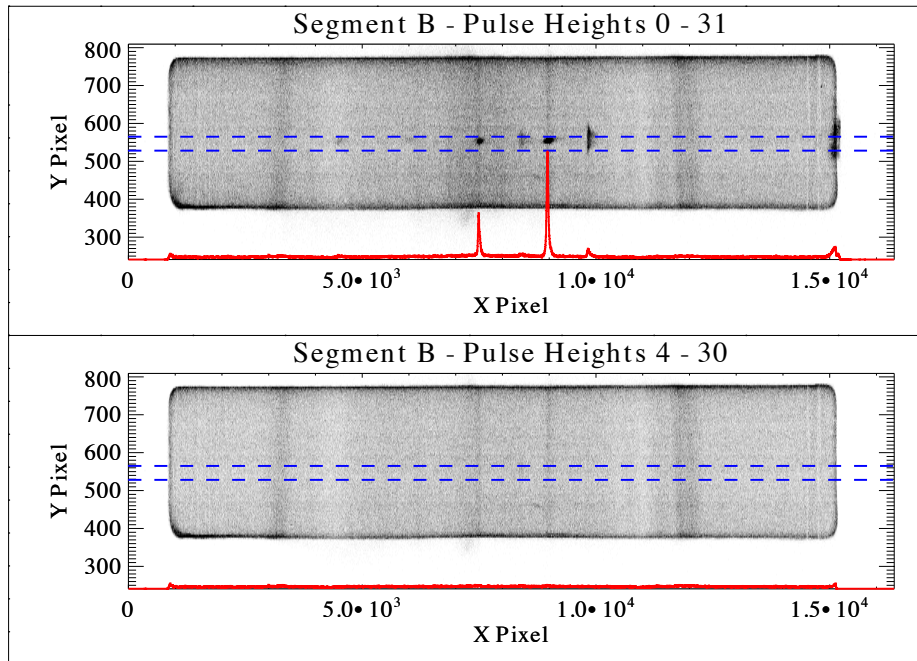


**Figure 7** Same as Figure 6, but for segment B. For this segment, the tighter pulse height threshold significantly reduces the prominent features.

No pulse height thresholding can be done in ACCUM mode, since the pulse height information is discarded onboard the spacecraft. However, only a small fraction of COS data is taken as ACCUMs, and these should all be exposures of very bright targets, where the background should have a negligible effect on the data.

#### **4.2 Long Term Count Rate vs. Time**

As described above, the dark rate was measured weekly in Cycle 17 as part of program 11895. Figure 8 shows the dark rate in a 300 pixel high region, centered around the spectrum, of each segment as a function of time since the launch of SM4. Times contaminated by close SAA passes have been excluded. From the figure it can be seen that the background rate has remained constant with time. As discussed above there is a spatial variation in the rate, so the exact value is a function of the area of the detector selected. By constructing histograms of the average dark rate per pixel, we have adopted a typical dark rate of  $\sim 1.5 - 2.0 \times 10^{-6}$  counts/sec/pixel, which is equivalent to  $< 1$  count/sec/cm<sup>2</sup>, or  $\sim 4 \times 10^{-4}$  counts/sec/resel (using the default extraction height). These values are consistent with the rate of 0.35 – 0.5 counts/sec/cm<sup>2</sup> ( $0.5 - 0.75 \times 10^{-6}$  counts/second/pixel) measured before launch.

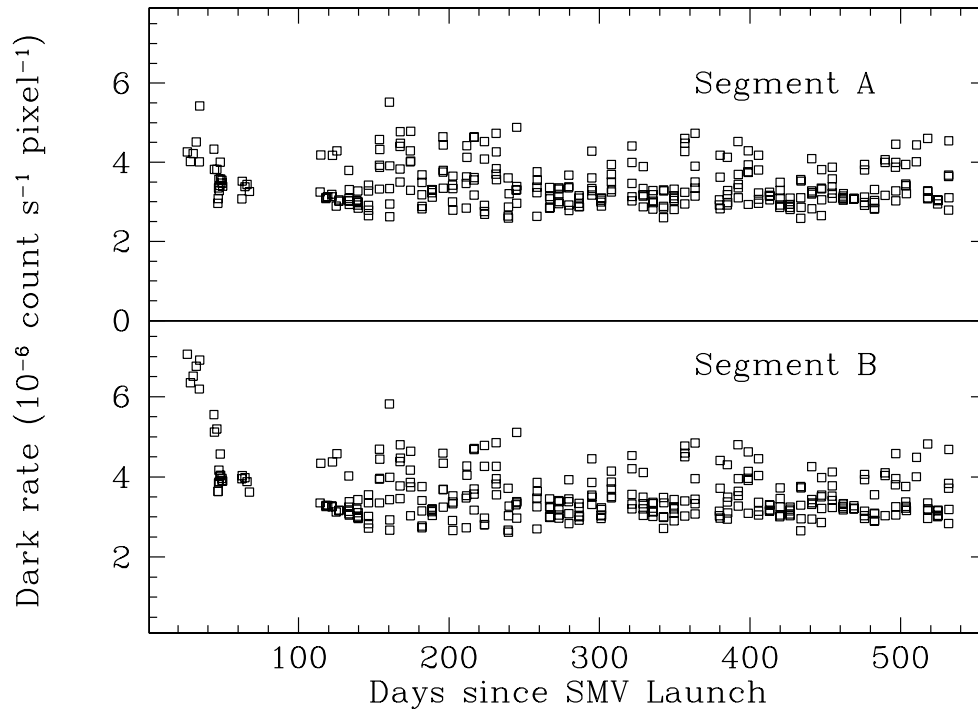


**Figure 8** Detector dark rate in a 300 pixel high area of the detector centered around the spectrum, using a pulse height range of 4 to 30; this rate has remained constant with time. Since the rate varies with position on the detector, the exact value depends on the region of the detector included.

## 5. Calcos and the background

Calcos determines the detector background for a particular exposure by measuring the total count rate in two background regions of the detector in that same exposure, using the identical pulse height threshold as for the science spectrum. The average count rate per pixel for the two regions is then scaled and subtracted from the extracted one-dimensional science spectrum. The XTRACTAB reference file (Shaw 2009) specifies the size and location of the background regions, which can be different for each segment, grating, and central wavelength. The advantage of this scheme is that any short-term temporal changes to the background which are uniform across the detector (such as that due to proximity to the SAA, for instance), will be properly accounted for. The disadvantage is that spatial variations are not addressed, so that any features that fall in the spectral extraction region will not be properly removed. In addition, any scattered light that falls in the background regions will result in oversubtraction of the background. A judicious choice of background region may be able to minimize the latter problem. Gain variation across the MCPs leads to incorrect results, since the background region will have different properties than the extraction regions.

## **6. Change History for COS ISR 2010-11**

Version 1: 07 October 2011 – Original Document

## **7. References**

Furst, F., et. al., 2009, *Earth and Planetary Science Letters*, 281, p 125.

McPhate, J., 2009, *Recommended COS FUV Detector Pulse Height Thresholds*, COS-090923-JBM.

McPhate, J., 2009, *COS FUV02 on-orbit behavior – Segment B “divot” and “clod”*, UCB memo COS-090731-JBM.

McPhate, J., et al., 2010, *COS FUV Detector Initial HV Turn On*, COS TIR 2010-02.

Sahnow, D., McPhate, J., Ake, T., Massa, D., Penton, S., Burgh, E., Zheng, W., 2011. On-Orbit Performance of the COS Detectors. *Proceedings of the 2010 STScI Calibration Workshop*. S. Deustua and C. Oliveira, eds, 386-393.

Sahnow, D., et al., 2011, *COS NUV Detector Dark Rates During SMOV and Cycle 17*, COS ISR-2011-12.

Shaw, B. et al. 2009 “COS Data Handbook”, Version 1.0, (Baltimore: STScI).

## Appendix

**Table 1: List of FUV Dark Exposures Affected by SAA**

<b>IPPPSOOT</b>	<b>DATE-OBS</b>	<b>Period affected (sec)</b>
LA8O01JZQ	30-Jun-2009	870
LA8O02BRQ	29-Jun-2009	630
LA8O03C0Q	29-Jun-2009	249
LA8O04SJQ	27-Jun-2009	159
LA8O05U5Q	27-Jun-2009	189
LA8O06VQQ	27-Jun-2009	660
LA8O07XLQ	27-Jun-2009	429
LA8O08XOQ	27-Jun-2009	249
LA8O09YSQ	28-Jun-2009	390
LA8O11AJQ	28-Jun-2009	309
LA8O12CYQ	3-Sep-2009	990
LA8O13ABQ	13-Jul-2009	90
LA8O15EOQ	16-Jul-2009	189
LA8O16LVQ	18-Jul-2009	990
LA8O18HVQ	6-Sep-2009	159
LA8O19I8Q	6-Sep-2009	990
LA8O20ISQ	3-Sep-2009	240
LA8O21GZQ	7-Sep-2009	870
LA8O22V5Q	10-Sep-2009	930
LA8O23VEQ	10-Sep-2009	579
LA8O24YMQ	11-Sep-2009	2139
LA8O25LCQ	13-Sep-2009	789
LB8S11LEQ	22-Sep-2009	939
LB8S1ZFHQ	9-Nov-2009	90
LB8S22G3Q	9-Nov-2009	150
LB8S2ICKQ	30-Nov-2009	399
LB8S2JJPQ	9-Dec-2009	90
LB8S30I8Q	29-Dec-2009	270
LB8S34LXQ	6-Jan-2010	189
LB8S3WFDQ	8-Feb-2010	219
LB8S4UCCQ	29-Mar-2010	279
LB8S5CAMQ	26-Apr-2010	570
LB8S6RDGQ	5-Jul-2010	90
LB8S71BVQ	19-Jul-2010	189
LB8S7AAXQ	2-Aug-2010	129